

# RELIABILITY-BASED NUMERICAL MODELING FOR INVESTIGATION OF THE IMPACT OF PRINTING PARAMETERS ON BUILDABILITY OF 3D PRINTED CONCRETE STRUCTURES

Meron Mengesha<sup>1,3,\*</sup>, Abrham Gebre<sup>3</sup>, Albrecht Schmidt<sup>2</sup>, Luise Göbel<sup>2</sup>, Tom Lahmer<sup>1,2</sup>

<sup>1</sup>Bauhaus-Universität Weimar, Germany, Institute of Structural Mechanics

<sup>2</sup>Materials Research and Testing Institute (MFPA) at Bauhaus-Universität Weimar, Germany

<sup>3</sup>School of Civil and Environmental Engineering Addis Ababa Institute of Technology, Addis Ababa University, Addis Ababa, Ethiopia

\*Corresponding author Email address: meron.wondafrash@gmail.com

DoI: <https://doi.org/10.20372/zede.v42i.10179>

## ABSTRACT

*The significance of 3D concrete printing (3DCP) as an additive manufacturing technology has increased over the past few years. Both academic research studies and large-scale industrial realizations of 3DCP have shown that it represents a viable alternative to traditional concrete mold casting. The key reason for this rapid development is that urgent challenges of the construction sector, in particular sustainability and productivity, are addressed. However, previous studies on technological progress have mainly been experimentally driven. The introduction of appropriate numerical modeling techniques would, therefore, further foster the success of 3DCP by providing insight into the structural behavior, which is beyond experimental possibilities. The present study introduces a numerical modeling technique for the analysis of 3DCP wall structures using a time-dependent reliability analysis. Uncertainties occurring throughout the printing process and time-dependent properties of printable concrete are considered. In addition, sensitivity analysis of random variables is done, which could be used as indicative preference for future process optimizations. The results yield valuable insight into the influence of printing process parameters on the failure of 3D printed concrete structures. The numerical model predicts build ability of a 3D printed concrete wall structure as it is in very good agreement with experimental results of similar studies.*

**Keywords:** 3D concrete printing, numerical

modeling, random variables, time-dependent reliability, build ability, sensitivity analysis

## 1. INTRODUCTION

Additive manufacturing refers to a procedure in which a product is created in layers using a computer-controlled positioning process based on a digital 3D model. Additive manufacturing and digital fabrication open up new possibilities in the production of concrete structures [1]. In contrast to traditional subtractive or forming production methods, additive manufacturing techniques allow for a design-driven manufacturing process, enabling the construction of structures with a high degree of complexity, design freedom, and functionality.

Among the different additive manufacturing technologies for concrete, extrusion-based techniques are supposed to be the most popular ones with a stringent entry into everyday construction processes [2-4] which offer material and labor savings, increased production speed, and complex geometries [1,5-7].

The reduced construction waste because of the accurately controlled manufacturing process of 3D printing and optimized material consumption may be estimated at 30 to 60 % [8]. The ability to construct concrete structures without the need for formwork has a significant economic and productivity benefit; as indicated by Perrot et al., formwork accounts for 35 to 60% of the total material costs in the construction industry [1].

Several challenges have been recognized that hamper the extension of 3DCP to a larger number of structural applications and to open its full potential with a load-bearing capacity. Fresh concrete undergoes time-dependent chemical reactions and rapid phase changes during the extrusion-based printing process. The material must be fluid in the first stage to be easily pumped towards the printing unit [3]. It is also commonly understood that the bonding strength of two consecutive layers reduces as the time gap between them increases [9].

Besides, variations in the properties of the raw materials, printing parameters, such as printing velocity, nozzle size, nozzle height from the printing platform, layer interval time, layer thickness, temperature and concrete mixture have a substantial effect on the overall performance of 3DPC [10-13]. Disturbances during printing may lead to inconsistencies and impair the quality of the product [14]. So-called cold joints should be avoided [15-17] by the appropriate setting of the printing process parameters. Insufficient strength, or stability may cause the 3DPC wall structure to fail during the process of printing, either by plastic yielding of the concrete (a strength mechanism) or due to elastic buckling of the printed height (a stability mechanism).

Several numerical modeling strategies to either simulate the extrusion process or estimate the printability of concrete objects have been developed. A first, finite element (FE) analysis of a 3D printed concrete shell construction was performed by Feng et al. [18]. Wolfs et al. [19] proposed a FE approach for a 3D printed concrete structure. A time-dependent Mohr-Coulomb failure criterion and a linear stress-strain behavior up to failure were used to investigate the failure mechanism of the structure.

Elastic buckling and plastic collapse were the two failure mechanisms investigated, as well as three different wall layouts (i.e., boundary conditions). As a result, the wall

that was simply supported showed global buckling, but the wall that is entirely clamped exhibits local buckling.

Comminal et al. [20] provided a computational fluid dynamics (CFD) model of 3DCP. The cross-sectional shape of 3D printed segments was predicted using numerical simulation. For a single layer printed on a planar build surface, the CFD approach can reliably model material extrusion and deposition.

The previously developed approaches for numerical models of the printing process have in common that they are deterministic in their nature. However, there are inherent uncertainties in the models' input parameters, mainly the elastic properties of the material phases due to raw materials or measurement uncertainties [21]. Large scatter on experimentally investigated freshly printed concrete specimens were observed [19, 22]. Therefore, a reliability-oriented model should account for both temporal changes and the randomness of material properties.

As a straight free wall buckles, it loses its stability and under goes large deformation necessitating for further investigation. Hence, in this study, modeling of a straight free wall with different layer thicknesses and wall widths is considered. Moreover, the findings of experimental tests are primarily focused on straight walls [8, 19, 23] and in this paper, these test data are used for validation. The present study introduces a numerical modeling approach for the assessment of the build ability of 3D printed concrete wall structures, in which a time-dependent reliability analysis is inserted. Various types of uncertainties throughout the printing process are taken into account by including the variability of printing process parameters. In addition, sensitivity analysis is used to evaluate the impact of various printing process parameters on the 3D printed concrete structures.

**2. METHODS**

**2.1. Numerical Modeling**

The 3D printed wall configuration used in this numerical model is the straight free wall. The defined boundary conditions are fixed at the bottom of the wall due to friction on the printed bed [19]. As the printing progresses, the loading consists of the increasing self-weight caused by the layer-wise production process.

**2.1.1. Specifics about the modeled concrete wall structure**

Mechanical properties of 3DPC, such as Young's modulus and compressive strength, exhibit considerable variations throughout the manufacturing process [19, 22]. During printing process, such variations on the properties of fresh concrete may result in geometrical imperfections [24]. Further uncertainties are related to the printing process itself, e.g., different printing velocities, varying time gaps between consecutive layers, and changing nozzle heights and pressures. Besides, interruptions during the printing

process may occur, resulting in further irregularities.

As a result, a simplified uncertainty approach is presented in this contribution, in which Young's modulus and compressive strength of freshly pumped concrete are modeled using log-normally distributed random processes [25]. Furthermore, random variables are used to represent printing process parameters such as printing velocity, wall length, width, thickness of each layer, and density. The statistical models of the random variables, as well as their corresponding distribution functions, are shown in Table 1. The mean and standard deviations of Young's modulus and compressive strength are obtained from Wolfs et al. [19]. An exponentially decaying correlation function with a layer-wise correlation structure with a correlation length of 30mm was assumed [25, 26]. The mean values and coefficients of variation of the other parameters have been obtained from recent studies [8,13,22, 27, 28]. The numerical simulation was realized by generating independent random numbers according to the considered distribution type and parameters [29-33].

**Table 1** Statistical distribution of the random variables

No.	Random variables	Mean values	CoV (%)	Min. value	Max. value	Distribution type
1	Young's modulus, $E(t)$ (kPa)	$1.2t+78$	15	$0.60t+39.5$	$1.80t+115.5$	Lognormal [29]
2	Compressive strength, $\sigma_v(t)$ (kPa)	$0.14t+5.98$	14	$0.08t+3.22$	$0.20t+8.73$	Lognormal [30]
3	Printing speed, $v_p$ (cm/s)	10.42	1.0	10.07	10.76	Normal [31]
4	Model Uncertainty, $N_R$	1.00	4.6	0.84	1.15	Lognormal [32]
5	Length, $L$ (mm)	1000	0.5	983.5	1,016.4	Normal [33]
6	Wall width, $\delta$ (mm)	55	3.0	49.57	60.5	Normal [33]
7	Thickness of each layer, $h$ (mm)	9.5	5.0	7.95	11.06	Normal [33]
8	Density, $\rho$ (kg/m <sup>3</sup> )	2033	0.56	1,994	2,072	Normal [32]

**2.1.2. Consideration of the time-dependent mechanical properties**

Because of the nature of the printing material and the specific process, some variations in the rheological properties of fresh concrete and the mechanical behavior

of the product must be accounted for [25]. This was also observed by [19, 22]. The time-dependent Young's modulus and compressive strength of concrete are given in Eqs. (1) and (2), respectively [19].

$$E(x,t) = E_0(x) + E_1t \tag{1}$$

$$\sigma_y(x,t) = \sigma_{y,0} + \sigma_{y,I} t \quad (2)$$

where:

$E_0(x)$  is the initial Young's modulus when it leaves the printing nozzle

$E_I$  is the gradient of temporal increment

$\sigma_{y,0}$  is the initial compressive strength of the printable concrete when it leaves the printing nozzle

$\sigma_{y,I}$  is the gradient of temporal increment

$t$  is the cycle time at a certain location  $x$

The time it takes to print a single layer is referred to as the layer cycle time. In an extrusion-based additive manufacturing of the wall, as shown in Figure1, the minimum layer cycle time for the  $i^{th}$  layer is determined using Eq. (3) [34].

$$t_i = H(x,t)/h \times (L/v_p) \quad (3)$$

where:

$v_p$  is the printing velocity

$H(x,t)$  is the total height at time  $t_i$  and a specific location  $x$

$L$  is the total travel length of the print head to extrude a single layer

$h$  is the thickness of a single layer

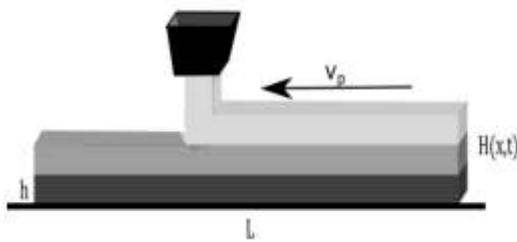


**Figure 1** Extrusion-based additive manufacturing of a wall of height  $H(x,t)$

A gradient of strength is formed over the height of the structure (Eqs. (1) to (3) [35]. This gradient is caused by the different layer cycles and hydration-induced micro-structural evolution of the concrete material after each layer is deposited [36]. In Figure1, the strength gradients are represented by shades of gray.

This gradient in strength was included in the proposed numerical model to investigate the stability of the extrusion-

based printed wall structure at any moment during the printing process. Regarding the temporal evolution of the compressive strength, Figure2 provides an example of the resulting strength gradient.

Following [19], an increase of  $\sigma_{y,I}=0.147$  kPa/min for the compressive strength, a printing velocity of 1cm/s is chosen for a concrete wall with a length of 500m, a width of 40mm, and a layer thickness of 9.5mm. Considering these variables, the gradient of the 3D printed concrete wall's strength produced by extrusion-based additive manufacturing is plotted and shown in Figure 2 [26].

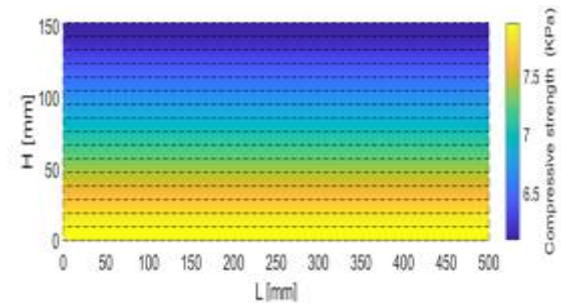


**Figure 2** Gradient of the strength of extrusion-based additive manufacturing of the concrete wall

## 2.2. Buildability in 3DCP Structures

The number of layers or the height at which the printed wall structure collapses is used to measure buildability [8]. Buildability depends upon the rheological properties of concrete; therefore, the simulation of the 3DCP process necessitates a choice of suitable material models. Buildability failure of printed wall structures has been described elsewhere [19,23] due to plastic collapse (a strength mechanism) and elastic buckling (a stability mechanism).

### 2.2.1. Elastic buckling

Another possible failure mode is the overall buckling of a slender vertical structure under its own weight,  $E_c(x,t)$ , can then be determined using Eq. (4) [37-39]. For the printed wall structure to be stable, the elastic Young's modulus has to stay higher than the critical value.

$$E_c(x,t) = H(x,t)^3 \rho g A / 8 I \quad (4)$$

where:

$I$  is the second moment of area

$A$  is the cross-sectional area

### 2.2.2. Plastic collapse

The plastic collapse of a 3D printed concrete wall structure is studied by comparing the stresses caused by concrete as expressed in Eq. (5)[34]:

$$\sigma_y(x,t) \leq \sigma_p(x,t) \quad (5)$$

where:

$\sigma_y(x,t)$  is the compressive yield strength

$\sigma_p(x,t)$  is the gravity-induced stresses

$\sigma_p(x,t)$  depends on the height of the wall to be printed and it can be written as expressed in Eq. (6) [36]:

$$\sigma_p(x,t) = \rho g H(x,t) \quad (6)$$

where:

$\rho$  is the density of the material

$g$  is the gravity

Another method for calculating gravity-induced stress is to use the printing elevation rate  $r$  as shown in Eq. (7) [34, 36, 37].

$$\sigma_p(x,t) = \rho g r t \quad (7)$$

The printing velocity and geometry of the wall structure to be printed (see Figure 1) define the elevation rate, Eq. (8) [34]:

$$r = v_p h/L \quad (8)$$

### 2.3. Reliability-based Assessment

Herein, a probability-based procedure is applied to ensure an appropriate safety margin. One advantage of using a probabilistic approach is that uncertain variables may be considered jointly and their effects may be separated systematically, which allows for a more

systematic determination of structural reliability [33].

The numerical model developed is able to estimate if a layered structure can support its self-weight and anticipate when it will collapse. The theoretical framework is based on comparing the vertical stress  $S(t)$  acting on the deposited layer to the critical stress  $R(t)$  associated with the material yield stress as described in section 2.2. The developed framework ensures that vertical stress does not reach critical stress [1].

In this study, a MATLAB algorithm was developed to compute the time-dependent vertical stress  $S(t)$ , critical stress  $R(t)$ , and design margin utilizing the statistical random variables mentioned in Table 1. As the printing progressed at each layer, 5000 combinations of random Latin Hypercube Sampling (LHS) variables were tested for reliability assessment.

#### 2.3.1. Time-dependent reliability

The material properties of the printed structure are functions of the hydration process. As a result, a time-dependent reliability assessment was used in the numerical simulation. The vertical stress gradually increases as successive layers are deposited in the extrusion-based additive manufacturing of concrete walls, and material strength properties evolve over time [10]. In order to assess reliability on a temporal scale, a straightforward idea is to utilize a generalization of the reliability equation in the time domain [29, 40-47]. As a result, the generalized reliability problem can be represented in Figure 3 for the 3DPC wall structure.

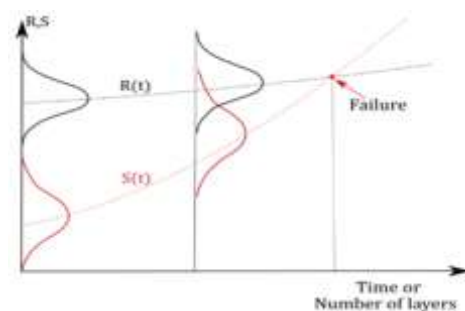


Figure 3 Time-dependency of both the resistance  $R(t)$  and load  $S(t)$  [40-44]

Whenever, at any point  $t$ , in the printing process, the safety margin  $M(t)$  is violated if the condition given in Eq. (9) is less than zero [29, 47].

$$M(t) = R(t) - S(t) < 0 \quad (9)$$

In this study, the reliability index was computed using the Rackwitz-Fiessler approach. As shown in Table 1, the resistance has a log-normal distribution and the load has a normal distribution. In these circumstances, the reliability index and the measure of the shift away from the mean value can be expressed by Eq. (10) [48].

$$\beta = \frac{\mu_R \left(1 - k \frac{\sigma_R}{\mu_R}\right) \left[1 - \ln \left(1 - k \frac{\sigma_R}{\mu_R}\right)\right] - \mu_S}{\sqrt{\left(\mu_R \left(1 - k \frac{\sigma_R}{\mu_R}\right) \left(\frac{\sigma_R}{\mu_R}\right)\right)^2 + \sigma_S^2}} \quad (10)$$

where:

$\beta$  is the reliability index

$\mu_R$  and  $\sigma_R$  are mean and standard deviation for the resistance, respectively

$\mu_S$  and  $\sigma_S$  are mean and standard deviation of total-load effect, respectively

$\bar{R}^e$ ,  $\sigma_R^e$  are mean and standard deviation for the resistance of the approximating normal distributions (equivalent normal parameters), respectively

$k$  is a multiplication factor of the standard deviation

The multiplication factor,  $k$  was computed using Eq. (11). The solution was determined iteratively by assuming a value for the design point and continues the iteration until  $\beta$  and  $x^*$  converge [48].

$$k = \frac{\mu_R - x^*}{\sigma_R} \quad (11)$$

where:

$x^*$  is the design point on the failure boundary.

Since no formwork was used to build the wall, failure was initiated if the safety margin tended to zero. In this case, the

factor of safety to be considered for the assessment of the buildability of the wall was fixed to one which is the condition where the critical stress  $R(t)$  and the vertical stress  $S(t)$  are equal. In this study, the minimum safety margin computed using Eq. (10) was considered zero. This resulted in a reliability index of zero which satisfied the minimum requirement to build the 3DPC wall. The reliability of the process decreased as the reliability index decreased.

Based on the concept of Eq. (9), the safety margins  $M(t)$  for elastic buckling and plastic collapse were computed according to Eq. (12) and Eq. (13), respectively.

$$M_E(t) = E(x, t) - N_R E_c(x, t) \quad (12)$$

$$M_p(t) = \sigma_y(x, t) - \sigma_p(x, t) \quad (13)$$

where:

$N_R$  is model uncertainty

### 2.3.2. Sensitivity analysis

Sensitivity analysis is the study of how the variation in the output of a statistical model can be attributed to different variations in the inputs of the model [49]. As there is a built-in MATLAB function developed [50], the sensitivity of the model to each of its input variables was assessed in this study using the Monte-Carlo based standard regression coefficients (SRC) [51,52]. In this method, the models given in Eq. (12) and Eq. (13) are approximated by a linear regression given in Eq. (14), with constants of  $b_0$  and  $b_i$ .

$$Y = M(X) \approx b_0 + \sum_{i=1}^n b_i X_i \quad (14)$$

The SRC indices are given in Eq. (15):

$$SRC_i = b_i \frac{\sigma_i}{\sigma_Y} \quad (15)$$

where:

$\sigma_x$  and  $\sigma_y$  denote the standard deviation of the model input  $X_i$  and the model output  $Y$ , respectively.

UQLab, an open-source scientific module for uncertainty quantification was used for the sensitivity analysis. For such tasks, a MATLAB built-in function for sensitivity analysis with a fixed Monte-Carlo sample size of 10,000 was used [50].

### 3. RESULTS AND DISCUSSION

#### 3.1. Time-Dependent Reliability Analysis Results

The time-dependent reliability analysis is used to assess the structure's susceptibility to failure during printing for the two types of failure mechanisms.

##### 3.1.1. Elastic buckling result

The critical Young's modulus at which buckling is expected to occur can be found by rearranging Eq. (4) for the considered one linear meter of a wall with a width ( $\delta$ ) and it is expressed by Eq. (16).

$$E_c(x,t) = 3 \rho g H(x,t)^3 / 2 \delta^2 \quad (16)$$

Figure 4 depicts the probability distributions of  $R(t)$  and  $S(t)$  for the overall buckling behavior of 3D printed concrete at each layer as a result of the time-dependent reliability analysis.

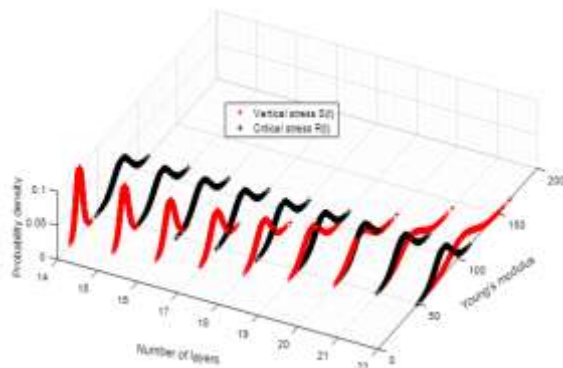


Figure 4 Probabilistic distribution of  $R(t)$  and  $S(t)$  for elastic buckling at different layers

The vertical stress as well as the critical stress, increases as the printing process progresses. As shown in Figure 4, the vertical stress due to self-weight is lower than the critical stress below layer 20, resulting in a safety margin of  $M(t) > 0$ , whereas after this layer, the vertical stress is greater than the critical stress, resulting in a safety margin of  $M(t) < 0$ , indicating that the printed wall begins to buckle.

Furthermore, Figure 5 provides the time-dependent reliability index graph for elastic buckling of a 3D concrete printed wall at each layer. As shown in Figure 5, as the number of layers increases, the reliability index decreases accordingly.

According to the time-dependent reliability analysis result, the maximum number of layers that can be printed without elastic buckling was found to be 20, as shown in Figures 4 and 5. This is in very good agreement with other experimental results of the research on 3D printing concrete [19, 23, 29, 53].

As seen in Figure 5, the reliability index declines steadily for the first 10 layers before rapidly reducing to zero beyond that. This is due to the fact that the elastic Young's modulus requirement (Eq. (16)) scales with the third power of height.

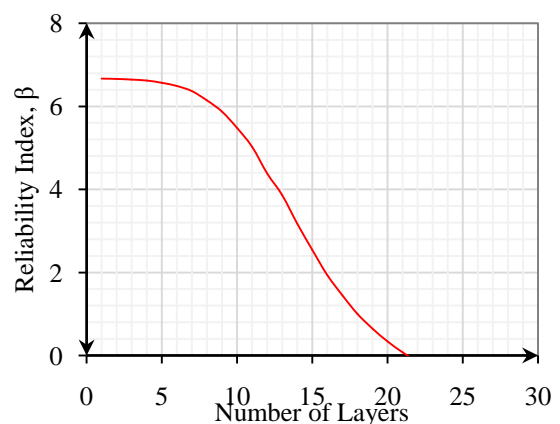
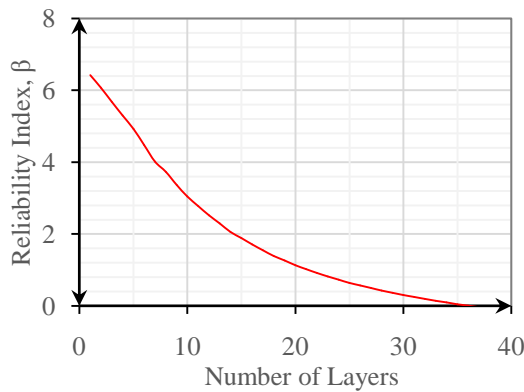


Figure 5 Time-dependent reliability index for elastic buckling of the 3DCP wall

##### 3.1.2. Plastic collapse result

Similarly, the time-dependent reliability index was determined for the plastic collapse using the inputs in Table 1. As

shown in Figure 6, after printing layer 36, the vertical stress is greater than the yielding stress, resulting in a safety margin  $M(t) < 0$ , indicating that the printed wall begins to collapse. The findings show that 3DPC wall printing is more prone to elastic buckling than plastic collapse due to self-weight, as various other studies have observed [8].



**Figure 6** Time-dependent reliability index for plastic collapse of the 3DPC wall

### 3.2. Sensitivity Analysis

As described before, the printing process parameters, in addition to the material composition, have significant impact on the final performance of 3DPC [12, 13, 54]. Printing process control and printing parameter selection are significant components that define the final printing quality of concrete, and they are also important linkages in the development of concrete 3D-printing structures [10].

Sensitivity analysis was carried out in order to identify the most sensitive parameter influencing the buildability of a 3D concrete printed wall. Furthermore, for the two types of failures, influential factors were identified and a parameter study was conducted. The relevant reliability indexes are computed as well.

#### 3.2.1. Sensitivity analysis for the elastic buckling

Sensitivity analysis of the printing process parameters on the elastic buckling safety margin function (Eq. (12)) in terms of sensitivity indices were computed at

5, 10, 15, and 20 layers. The first printed layer was referred to as layer 1, and so on.

The comparison of the sensitivity indices of printing process parameters is shown in Figure 7. In the early stages, variations in the printing speed have the largest impact on the stability. In contrast, later on, the variability of width and layer thickness have a greater impact on the buildability of 3D printed concrete. The important effect of the width on buildability has also been illustrated in [37]. The influence of the printing speed reduces after the tenth layer, as seen in Figure 7. After the fifteenth layer, the wall width and layer thickness have the most significant influences on the stability of the 3DPC wall structure.

Variability in the layer thickness has negative effects on the wall's stability, whereas variation in the width has positive consequences. This means that increasing the layer thickness reduces the elastic buckling resistance and increasing the wall width increases elastic buckling resistance. The length and density variables, in particular, exhibit lower significance and low sensitivity, implying that, if necessary, these variables might be considered constants in the elastic buckling analysis.

#### 3.2.2. Sensitivity analysis for the plastic collapse

Similarly, at selected layers 5, 10, 15, 20, 25 and 30, sensitivity analysis of printing process parameters on the plastic collapse safety margin function (Eq. (13)) in terms of sensitivity indices were computed. The variations of the printing speed as well as the layer thickness contribute more to the plastic collapse in the early and later stages compared to the elastic buckling analysis, as shown in Figure 8. Variability in both printing parameters has an adverse influence on the plastic collapse resistance, implying that raising these printing process parameters reduces the resistance to plastic collapse. The reason for this may be that increasing the printing velocity decreases the layer cycle time while raising the layer height increases the wall's self-weight. The length and density variables are less



influential input parameters in the plastic collapse analysis, contributing less to the

variability of the results.

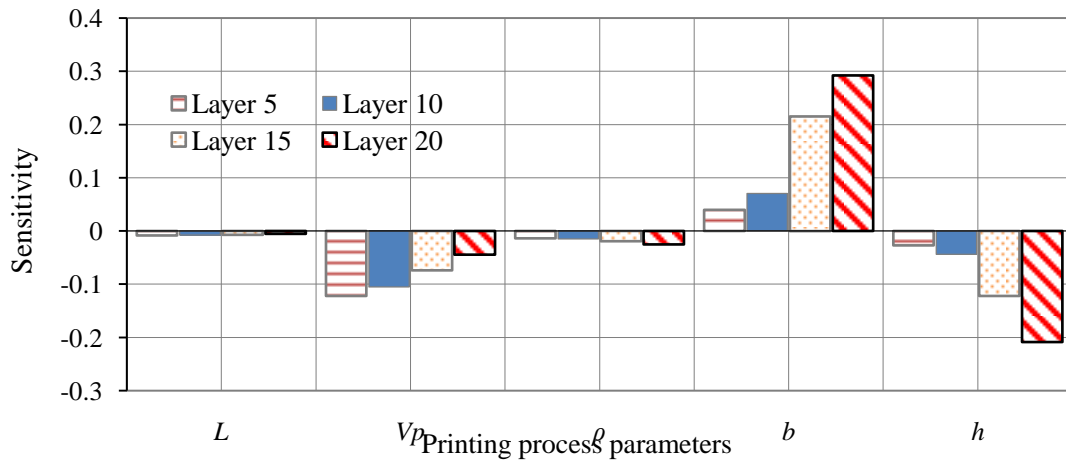


Figure 7 Sensitivity of printing process parameters on the elastic buckling safety margin function

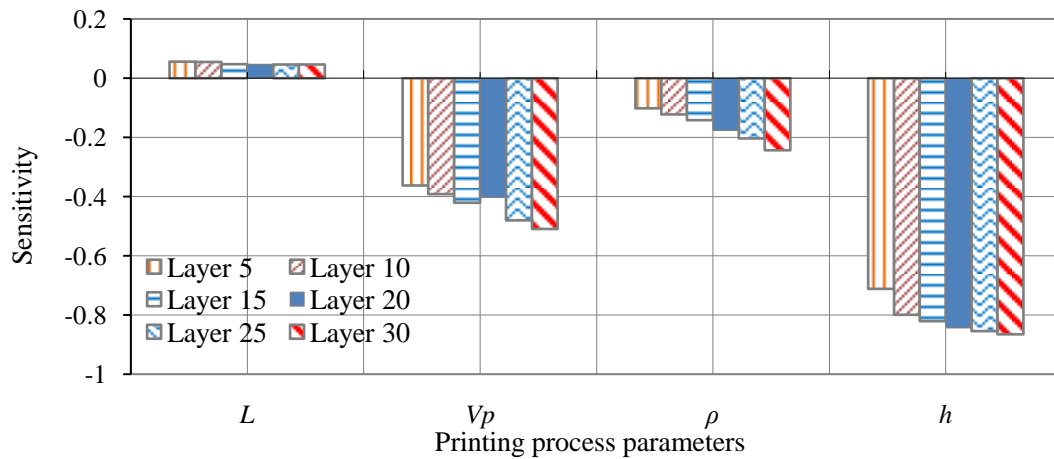


Figure 8 Sensitivity of printing process parameters on the plastic collapse safety margin function

### 3.3. Parametric Study

The influence of printing process parameters on the contribution to the variability of the stability of 3DPC walls is investigated further. Based on the sensitivity analysis results, the wall width and layer thickness for the case of elastic buckling, as well as the printing velocity and layer thickness for plastic collapse, were chosen for the following parameter study.

#### 3.3.1. Elastic buckling

##### i. Effect of layer thickness

The MATLAB algorithm was used to conduct the time-dependent reliability

study, and the layer thicknesses chosen were based on a majority of studies done on the 3DCP projects [53]. Figure 9 shows the effect of layer thickness on  $\beta$ . In the analysis, other parameters were considered as deterministic values (i.e.,  $v_p=10.42$  cm/s,  $b=55$  mm and  $L=1000$  mm). Lowering the layer thickness increases the buildability height, as seen in Figure 9. For example, a layer thickness of 8 mm increases the wall height by 8.27 % when compared to a layer thickness of 9.5 mm.

This is also expected because lowering the layer thickness increases the overall buildability time (Eq. (3)), which increases the concrete material yielding strength (Eq. (1)). Similarly, increasing the layer thickness reduces the wall's buildability

height. For example, a layer thickness of 15 mm reduces the total buildability height by 13.53 % when compared to a 9.5 mm layer thickness.

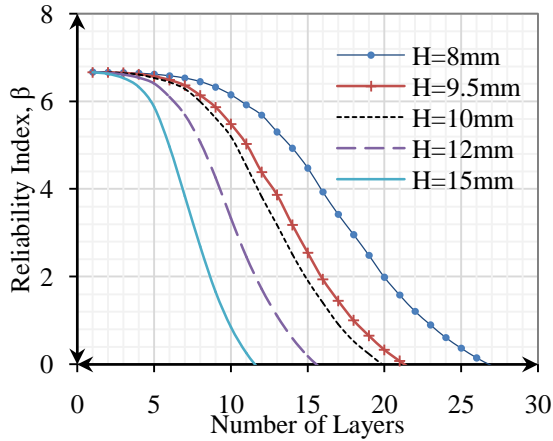


**Figure 9** Time-dependent reliability index for 3D printed concrete with different layer thicknesses

**i. Effect of wall width**

Similarly, to the previous section, ranges of wall width were chosen based on the previously reported values [55]. As demonstrated in Figure10, increasing the wall width results in a higher buildability height, which is similar to the finding obtained elsewhere [37]. The buildability height increases by more than 80% when the maximum and minimum widths of the selected wall widths ( $w$ ) are compared. This is because increasing the width of the wall increases its stiffness, which reduces the loss of stability [8].

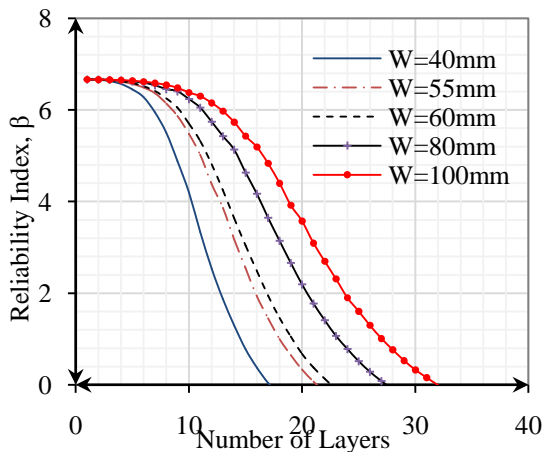


**Figure 10** Time-dependent reliability index for 3D printing concrete with different wall widths

**3.3.2. Plastic collapse**

The printing velocity and the layer thickness are the most influential parameters for the plastic collapse, according to the sensitivity analysis. By keeping the other printing process parameters constant and just altering the printing speed and layer thickness, a parameter study was performed and the results are shown in the next sections.

**i. Effect of printing velocity**

The influence of the printing speed on 3D printing plastic collapse is substantial at lower speeds (1.2cm/s), which can produce concrete with around 80 layers, as demonstrated in Figure11.

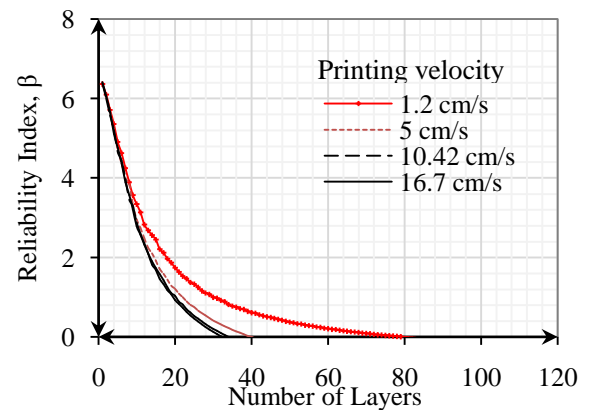


**Figure 11** Time-dependent reliability indexes for 3D printing concrete with different printing speeds

Because of the high increase in the layer cycle time (Eq. (3)), along with the reduction of the printing speed from 16.7 cm/s to 1.2 cm/s, the height before plastic collapse rises by over 85 % .

**ii. Effect of layer thickness**

For the next parameters study, the same layer thickness as used in section 3.3.1 was employed. When the layer thickness is reduced from 15 mm to 8 mm, the height of the wall increases by 6.67 % before the plastic collapses, as illustrated in Figure12. The reason for this is that decreasing the layer thickness increases the layer cycle

time, which increases the yielding strength.

The results revealed that the printing velocity variability has a greater impact on the plastic collapse than layer thickness.

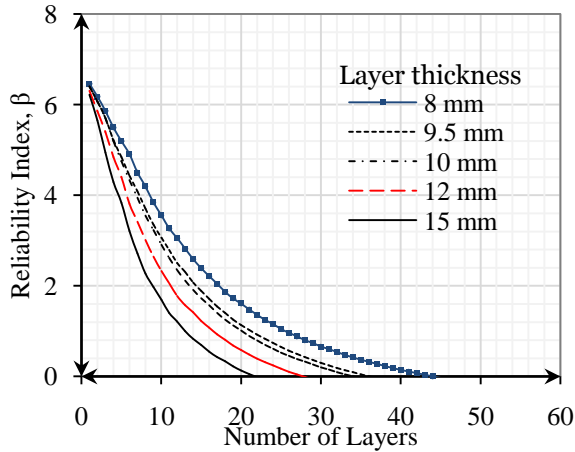


**Figure 12** Time-dependent reliability index for 3D printing concrete with different layer thicknesses

#### 4. CONCLUSIONS

A reliability-based assessment scheme considering the variability of printing process parameters for the buildability of 3D concrete is presented.

According to reliability and sensitivity analysis, changes in printing speed, layer thickness, and concrete width are the most influential parameters for predicting the maximum number of printed concrete layers before failure. It is also noted that after the wall tends to buckle, reducing the printing speed of the 3DCP does not have an impact on its buckling stability. The sensitivity results revealed that the printing velocity variability has a greater impact on the plastic collapse than the layer thickness. Furthermore, the elastic buckling is influenced more by the width of the concrete wall than by the thickness of the layers.

Plastic collapse is influenced more by the printing speed than elastic buckling is, and elastic buckling is influenced more by the width of the concrete wall than plastic collapse is.

The length and the density variables, in particular, exhibit lower significance and low sensitivity, implying that, if necessary, these variables might be considered constants in the elastic buckling analysis and plastic collapse.

#### CONFLICT OF INTEREST

The authors declare that there is no conflict of interest.

#### ACKNOWLEDGMENTS

The work has been financially supported by different institutions, which is highly acknowledged. Among them are DAAD (Ethiopian - German Exchange of Ph.D. candidates), DFG (German Research Foundation) within the priority program 1886 “Polymorphic uncertainty modeling for the numerical design of structures” and the Federal State of Thuringia, Germany.

#### REFERENCES

- [1] Perrot, A., Rangeard, D., and Pierre, A., “*Structural Built-up of Cement-based Materials used for 3D-Printing Extrusion Techniques*”, *Materials and Structures*, vol. 49, no. 4, 2016, pp. 1213–1220, doi: 10.1617/s11527-015-0571-0.
- [2] Valente, M., Sibai A., and Sambucci, M., “*Extrusion-based Additive Manufacturing of Concrete Products: Revolutionizing and Remodeling the Construction Industry*”, *Journal of Composites Science*, vol 3, no. 3, 2019, pp. 1-20, doi:10.3390/jcs3030088.
- [3] De Schutter, G., Lesage, K., Mechtcherine, V., Nerella, V. N., Habert, G., and AgustiJuan, I., “*Vision of 3D Printing with Concrete-Technical, Economic and Environmental Potentials*”, *Cement and Concrete Research*, vol. 112, 2018, pp.25–36, doi.org/10.1016/j.cemconres.2018.06.001

- [4] Albar, A., Chougan, M., Al- Kheetan, M. J., Swash, M. R., and Ghaffar, S. H., “*Effective Extrusion-based 3D Printing System Design for Cementitious-based Materials*”, *Results in Engineering*, vol. 6, 2020. doi.org/10.1016/j.rineng.2020.100135.
- [5] Chen, Y., Veer, F., and Copuroglu, O., “*A Critical Review of 3D Concrete Printing as a Low CO<sub>2</sub> Concrete Approach*”, *Heron*, vol. 62 no. 3, 2017, pp. 167-194. doi:10.13140/RG.2.2.12323.71205.
- [6] Bos, F., Wolfs, R., Ahmed, Z. and Salet, T., “*Additive Manufacturing of Concrete in Construction: Potentials and Challenges of 3D Concrete Printing*”, *Virtual and Physical Prototyping*, vol. 11, no. 3, 2016, pp. 209-225. doi:10.1080/17452759.2016.1209867
- [7] Hojati, M., Li, Z., Memari, A. M., Park, K., Zahabi, M., Nazarian, S., Duarte, J. P., and Radlińska, A., “*3D-Printable Quaternary Cementitious Materials Towards Sustainable Development: Mixture Design and Mechanical Properties*”, *Results in Engineering*, vol. 13, 2022. doi.org/10.1016/j.rineng.2022.100341.
- [8] Kaszyńska, M., Skibicki, S., and Hoffmann, M., “*3D Concrete Printing for Sustainable Construction*”, *Energies*, vol. 13, no. 23, 2020, doi.org/10.3390/en13236351.
- [9] Le, T.T., Austin, S.A., Lim, S., Buswell, R.A., Law, R., Gibb, A.G., and Thorpe, T., “*Hardened Properties of High-Performance Printing Concrete*”, *Cement and Concrete Research*, vol. 42 no. 3, 2012, pp. 558–566.
- [10] Fuyan, L., Zhao, D., Hou, X., Sun, L., and Zhang, Q., “*Overview of the Development of 3D-Printing Concrete: A Review*”, *Applied Sciences*, vol. 11, no. 21, 2021. doi.org/10.3390/app11219822.
- [11] Uzel, S.G., Weeks, R.D., Eriksson, M., Kokkinis, D. and Lewis, J.A., “*Multi-material Multi-nozzle Adaptive 3D Printing of Soft Materials*”, *Advanced Materials Technologies*, vol. 7, no. 8, 2022, pp. 1-10.
- [12] Khan, M. S., Sanchez, F., and Zhou, H., “*3-D Printing of Concrete: Beyond Horizons*”, *Cement and Concrete Research*, vol. 133, 2020, doi.org/10.1016/j.cemconres.2020.106070.
- [13] Rehman, A. U., and Kim, J.H., “*3D Concrete Printing: A Systematic Review of Rheology*”, *In Materials*, vol. 14, no. 14, 2021, doi.org/10.3390/ma14143800.
- [14] Buswell, R. , Leal de Silva, W. Jones, S. and Dirrenberger, J., “*3D printing using Concrete Extrusion: A Roadmap for Research*”. *Cement and Concrete Research*, vol. 112, 2018, pp. 37-49, doi.org/10.1016/j.cemconres.2018.05.006.
- [15] Nerella, V., Hempel, S. and Mechtcherine, V., “*Effects of Layer-Interface Properties on Mechanical Performance of Concrete Elements Produced by Extrusion-Based 3D Printing*”, *Preprints*, 2018. doi.org/10.20944/preprints201810.0067
- [16] Panda, B. , Paul, S. C. , Mohamed, N. A. N. ,Tay, Y. W. D. and Tan, M. J., “*Measurement of Tensile Bond Strength of 3D Printed Geopolymer Mortar*”, *Measurement*, vol. 113, 2018, pp. 108-116. doi.org/10.1080/17452759.2018.1500420.
- [17] Lee, H., Kim, J. J., Moon, J., Kim, W., and Seo, E., “*Evaluation of the Mechanical Properties of a 3D-Printed Mortar*”, *Materials*, vol. 12, no. 24, 2019, pp. 1–13.
- [18] Feng, P. , Meng, X.Chen, J.F. and Ye, L., “*Mechanical Properties of Structures 3D Printed with Cementitious Powders*”, *Construction*

- and Building Materials, vol. 93, 2015, pp. 486-497.  
doi:10.1016/j.conbuildmat.2015.05.132
- [19] Wolfs, R., Bos, F. and Salet, T., “*Early Age Mechanical Behaviour of 3D Printed Concrete: Numerical Modelling and Experimental Testing*”, Cement and Concrete Research, vol. 106, 2018, pp. 103-116, doi.org/10.1016/j.cemconres.2018.02.001.
- [20] Comminal, R., Leal da Silva, W. R., Andersen, T. J., Stang, H., and Spangenberg, J., “*Modelling of 3D Concrete Printing based on Computational Fluid Dynamics*”, Cement and Concrete Research, vol. 138, 2019.  
doi.org/10.1016/j.cemconres.2020.106256
- [21] Göbel, L., Lahmer, T., & Osburg, A., “*Uncertainty Analysis In Multiscale Modeling of Concrete based on Continuum Micromechanics*”, European Journal of Mechanics, A/Solids, vol. 65, 2017, pp. 14–29, doi.org/10.1016/j.euromechsol.2017.02.008.
- [22] Casagrande, L., Esposito, L., Menna, C., Asprone, D., and Auricchio, F., “*Effect of Testing Procedures on Buildability Properties Of 3D-Printable Concrete*”, Construction and Building Materials, vol. 245, 2020, doi.org/10.1016/j.conbuildmat.2020.118286.
- [23] Suiker, A. S. J., “*Mechanical Performance of Wall Structures in 3D Printing Processes: Theory, Design Tools and Experiments*”, International Journal of Mechanical Sciences, vol. 137, 2018, pp. 145-170.  
doi.org/10.1016/j.ijmecsci.2018.01.010.
- [24] Buswell, R. , Kinnell, P. , Xu, J. , Hack Kloft, H, Maboudi, M. , Gerke, M., Massin, P. Grasser, G. , Wolfs, R.J.M., and Bos, F.P., “*Inspection Methods for 3D Concrete Printing*”, 2<sup>nd</sup> RILEM International Conference on Concrete and Digital Fabrication: Digital Concrete 2020, vol. 28, 2020, pp. 790–803.
- [25] Schmidt, A., Mengesha, M., Göbel, L., Könke, C., Lahmer, T., “*Numerical Modeling of an Extrusion-based Concrete Printing Process Considering Spatially and Temporarily Varying Material and Process Parameters*”, 18<sup>th</sup> International Probabilistic Workshop, vol 153, 2021, pp. 531-538.
- [26] Mengesha, M., Schmidt, A., Göbel, L., Lahmer, T., & Könke, C., “*Numerical Simulation for 3D Printed Wall Structure During the Process of Printing Considering Uncertainty*”, 4<sup>th</sup> International Conference on Uncertainty Quantification in Computational Sciences and Engineering, 2022, pp. 100–111, doi: 10.7712/120221.8025.18985.
- [27] Wolfs, R. J. M., and Suiker, A. S. J., “*Structural Failure During Extrusion-based 3D Printing Processes*”, International Journal of Advanced Manufacturing Technology, vol. 104, 2019, pp. 565–584.  
doi.org/10.1007/s00170-019-03844-6.
- [28] Wolfs, R. J. M., Bos, F. P., and Salet, T. A. M., “*Triaxial Compression Testing on Early Age Concrete for Numerical Analysis of 3D Concrete Printing*”. Cement and Concrete Composites, vol. 104, 2019, doi.org/10.1016/j.cemconcomp.2019.103344.
- [29] Gordon A., Fenton, D. and Griffiths, V., “*Risk Assessment in Geotechnical Engineering*”, John Wiley & Sons, 2008.
- [30] Baji, H., and Yang, W., “*Probabilistic Model for Time to Cover Cracking due to Corrosion*”. Structural Concrete, vol. 21, no. 4, 2019, pp. 1408-1424, doi.org/10.1002/suco.201900341.
- [31] Pradalier, C. , Hermsillo, J. , Koike, C., Braillon, C., Bessire, P. and

- Laugier, C., “*Safe and Autonomous Navigation for a Car-Like Robot among sPedestrian*”, Int. Workshop on Service, Assistive and Personal Robots, Madrid (ES), 2003.
- [32] NCHRP REPORT 292, “*Strength Evaluation of Existing Reinforced Concrete Bridges*”, Transportation Research Board, Washington DC, 1987.
- [33] JCSS “*Probabilistic Model Code, Part 1-Basis of Design*”, Joint Committee on Structural Safety, 2000, pp. 64.
- [34] Perrot, A. and Rangeard, D., “*3D Printing in Concrete: Techniques for Extrusion/Casting, State of the Art and Challenges of the Digital Construction Revolution*”, 2019, pp. 41-72, doi: 10.1002/9781119610755.
- [35] Mengesha, M., Schmidt, A., Göbel, L., Lahmer, T., “*Numerical Modeling of an Extrusion-based 3D Concrete Printing Process Considering a Spatially Varying Pseudo-Density Approach*, 2<sup>nd</sup> RILEM International Conference on Concrete and Digital Fabrication, 2020, doi:10.1007/978-3-030-49916-7\_33.
- [36] Perrot, A., “*3D Printing of Concrete*”, ISTE Ltd and John Wiley & Sons, Inc, Great Britain and the United States, 1<sup>st</sup> ed. 2019, doi:10.1002/9781119610755.
- [37] Roussel, N., “*Rheological Requirements for Printable Concretes*”, Cement and Concrete Research, vol. 112, 2018, pp. 76-85, doi.org/10.1016/j.cemconres.2018.04.005.
- [38] Esposito, L., Menna, C., Asprone, D., Rossino, C., Marchi, M., “*An Experimental Testing Procedure to Assess the Buildability Performance of 3D Printed Concrete Elements*”. 2<sup>nd</sup> RILEM International Conference on Concrete and Digital Fabrication. vol 28. Springer, 2020, doi: 10.1007/978-3-030-49916-7\_24.
- [39] Greenhill, A., “*Determination of the Greatest Height Consistent with Stability that a Vertical Pole or Mast can be Made, and of the Greatest Height to which a Tree of Given Proportions can Grow*”, In Proceedings of the Cambridge Philosophical Society, vol. 4, 1881.
- [40] Wang, C., “*Structural Reliability and Time-Dependent Reliability*”, Springer Nature, Switzerland, 2021, doi: 10.1007/978-3-030-62505-4.
- [41] Wen, Y. K., and Chen, H. C., “*On Fast Integration for Time Variant Structural Reliability*”, Probabilistic Engineering Mechanics, vol. 2, no. 3, 1987, pp. 156–162.
- [42] Baingo, D. A., “*Framework for Stochastic Finite Element Analysis of Reinforced Concrete Beams Affected by Reinforcement Corrosion*”, (Doctoral dissertation), University of Ottawa, 2012.
- [43] Rostam, S., “*Reinforced concrete Structures - Shall Concrete Remain the Dominating Means of Corrosion Prevention?*”, Materials and Corrosion, vol. 54, no. 6, 2003, pp. 369–378, doi.org/10.1002/maco.200390086.
- [44] Siemes, T., and Rostam, S., “*Durable Safety and Serviceability: A Performance based Design Format*”, IABSE Colloquium, 1996, pp. 41–50.
- [45] Stewart, M. G., and Rosowsky, D. V., “*Structural Safety and Serviceability of Concrete Bridges Subject to Corrosion*”, Journal of Infrastructure Systems, vol. 4, no. 4, 1998, pp.146–155.
- [46] Animesh, D., and Sankaran, M., “*Reliability Estimation with Time-Variant Loads and Resistances*”, Journal of Structural Engineering, vol. 126, 2000, pp. 612–620.
- [47] Melchers, R. E., and Beck, A. T., “*Structural Reliability-Analysis and*

- Prediction*”, 3<sup>rd</sup> ed., John Wiley & Sons Ltd. 2018.
- [48] Ghasemi, S. H., and Nowak, A. S., “*Reliability Index for Non-Normal Distributions of Limit State Functions*”, *Structural Engineering and Mechanics*, vol. 62, no. 3, 2017, pp. 365–372, doi.org/10.12989/sem.2017.62.3.365.
- [49] Saltelli, A., Tarantola, S., and Campolongo, F., “*Sensitivity Analysis as an Ingredient of Modeling*”, *Statistical Science*, vol. 15, no. 4, 2000, pp. 377–395.
- [50] Marelli, S., Lamas, C., Konakli, K., Mylonas, C., Wiederkehr, P. and Sudret, B., “*UQLab User Manual-Sensitivity Analysis*”, *Report UQLab-VI*, 2019, pp.2-106.
- [51] Saltelli, A., and Marivoet, J., “*Non-Parametric Statistics in Sensitivity Analysis for Model Output: A Comparison of Selected Techniques*”, *Reliability Engineering and System Safety*, vol. 28, no. 2, 1990, pp. 229–253.
- [52] Borgonovo, E., and Plischke, E., “*Sensitivity Analysis: A Review of Recent Advances*”, *European Journal of Operational Research*, vol. 248, no. 3, 2016, pp. 869–887.
- [53] Suiker, A. S. J., “*Effect of Accelerated Curing and Layer Deformations on Structural Failure during Extrusion-based 3D Printing*”, *Cement and Concrete Research*, vol. 151, 2022, doi.org/10.1016/j.cemconres.2021.106586.
- [54] Li, Z., Hojati, M., Wu, Z., Piasente, J., Ashrafi, N., Duarte, J. P., Nazarian, S., Bilén, S. G., Memari, A. M., and Radlińska, A., “*Fresh and Hardened Properties of Extrusion based 3D-Printed Cementitious Materials: A Review*”, *Sustainability*, vol. 12, no. 14, 2020, pp. 1–33. doi.org/10.3390/su12145628.
- [55] Kruger, J., Cho, S., Zeranka, S., Viljoen, C., and van Zijl, G., “*3D Concrete Printer Parameter Optimisation for High Rate Digital Construction Avoiding Plastic Collapse*”, *Composites Part B: Engineering*, vol. 183, 2020, doi.org/10.1016/j.compositesb.2019.107660.